J Therm Anal Calorim (2012) 108:933–938
DOI 10.1007/s10973-012-2412-5

Thermal conductivity of polyurethane composites containing nanometer- and micrometer-sized silver particles

Muhammad Iqbal · Michael McCullough · Adam Harris · S. Holger Eichhorn

CTAS2011 Conference Special Chapter

Abstract Polyurethane composites containing spherical and flake-shaped silver fillers of micrometer and nanometer sizes were prepared by reacting suspensions of the silver filler in tetraethylene glycol with Desmodur® HL BA. Both the thermal conductivity and the stability of the silver composites are increased in comparison with a reference polyurethane sample without filler. Unexpectedly, the largest increases in thermal conductivity and stability are observed for the spherical silver particles of micrometer size but not for the silver nanoparticles, which is reasoned with larger aggregates of silver particles and a higher degree of crystallinity in the sample containing micrometer-sized silver particles.

Keywords Thermal conductivity · Polyurethanes · Polymer composites · Silver nanoparticles · TG · DSC · SEM · Silver composites · Nanoparticles

Introduction

Thermal conductivity of plastics is an important design parameter for applications that require the dissipation of heat generated by components, such as microprocessors, power semiconductors, high power RF devices, laser diodes, LEDs, and MEMS. Intense research efforts over the last decade have led to the development of a range of high-performance thermal materials. These materials can be categorized into monolithic materials, carbonaceous materials, metal matrix composites, ceramic matrix composites, carbon/carbon composites, and polymer matrix composites (PMCs) [1–7]. The main advantages of PMCs are their relatively low density and established processing methods. PMCs containing metal or ceramic particles are widely used in the electronics industry as underfills, encapsulants, and thermal interface materials such as thermally conductive adhesives [1–7].

Thermal conductivity, in contrast to electrical conductivity, of PMCs containing metal/metal oxide particles has been given little attention in the scientific literature despite its important industrial applications. Reported experimental and theoretical studies have shown that the thermal conductivity of PMCs depends especially on the shapes and distribution of aggregates formed by the conductive filler, which is a function of the size and the morphology (e.g., spheres, flakes, short fibers, rods, and tubes) of the filler material, the processing method, and the type of polymer matrix [4, 8, 9]. Aggregation of the filler into dendritic chains rather than clusters, for example, resulted in exponential increases in thermal conductivity with increasing filler concentration because continuous conductive pathways are created more efficiently [10]. Thermal interfacial resistance has been determined as another important factor that controls thermal conductivity in PMCs. Interfacial resistance may be particularly high when nanometer-sized metal fillers are applied because their surfaces more easily oxidize in air or are protected by organic compounds [11].

However, experimental studies especially on the thermal conductivity of PMCs containing metal/metal oxide fillers are scarce. Polyurethanes (PUs) containing metal/metal oxide fillers have received some attention but all of the reported studies focus on the improvement of properties

M. Iqbal · S. H. Eichhorn (✉)
Department of Chemistry and Biochemistry, University of Windsor, Windsor, ON, Canada
e-mail: eichhorn@uwindsor.ca

M. McCullough · A. Harris
C-Therm Technologies Ltd, C/O RPC 921 College Hill Road, Fredericton, NB, Canada

other than thermal conductivity, such as mechanical [12, 13], thermal [12, 14], biostability [15], and antimicrobial properties [16]. Raja et al. [17] reported increases of thermal and electrical conductivities of PU composites containing increasing amounts (1–5 wt%) of carbon nanotubes that were decorated with silver and copper nanoparticles but the main focus of this study was on shape memory effects.

Presented in this article is a comparative study of the thermal conductivity of PU composites containing spherical silver particles of micro- and nanometer sizes as well as silver flakes of micrometer size. The silver contents of all the samples were kept constant at 15 wt% to probe the effect of the size and shape of the silver fillers on the thermal conductivity and other thermal properties of the composite materials.

Experimental

Materials and synthesis

Ag microparticles, as spherical powders (0.5–1 μm) and as flakes (1–3 μm), were purchased from STREM Chemicals, while Ag nanoparticles of three different sizes (20–30 nm, 50–60 nm, and 90–100 nm) were purchased from Sky-Spring Nanomaterials. All Ag fillers were used as received. Desmodur® HL BA was provided by Bayer Materials Science, Canada and consists of a mixture of aliphatic and aromatic diisocyanates in butyl acetate (60 wt% non-volatile content), which were reacted with tetraethylene glycol (TEG) (Sigma-Aldrich). All solvents were of either HPLC grade or obtained from a Grubbs' type solvent purification system by Innovative Technology®.

PU silver (**PU–Ag**) composites were prepared by mixing Desmodur® HL BA (NCO content = 10.5 ± 0.5 wt%) with TEG in a 1:1 molar ratio of NCO to OH content. The as-received solution of Desmodur® HL BA was diluted by mixing it with ethyl acetate in a 3:7 ratio by weight before it was combined with TEG and filler. All amounts of Ag fillers were calculated to provide an Ag content of 15 wt% with respect to the combined amounts of Desmodur® HL BA (non-volatile content) and TEG. Ag particles and flakes were mixed with the required amount of TEG and sonicated before being mixed with the diluted solution of Desmodur® HL BA.

After combining all components, the mixtures were sonicated for another 2–3 min and then stirred to maintain a good dispersion of the Ag particles. When the mixtures became too viscous for stirring with a magnetic stir bar (5–7 min after mixing), they were cast into PTFE molds and allowed to set. The samples were first cured at 60 °C for 1 h, then at 125 °C for 2 h, and finally dried under high vacuum (30 millitorr) for 3 h to ensure proper setting and complete removal of solvents. Removal of the polymer composites from the PTFE molds gave disks of 18–20 mm diameter and 3–5 mm width (Scheme 1). The samples are designated based on the type of polymer-filler. Addition of Ag flakes or powders with diameters of 0.5–1 μm, 90–100 nm, 50–60 nm, and 20–30 nm yield samples of **PU–Ag (flakes)**: **PU–Ag (0.8 μm)**, **PU–Ag (95 nm)**, **PU–Ag (55 nm)**, and **PU–Ag (25 nm)**, respectively. Reference PU sample **PU (ref)** was prepared by the same procedure, but no Ag filler was added.

Characterization

Thermal gravimetric analysis was conducted on a Mettler Toledo TG SDTA 851e. Samples were stored at 25 °C for 30 min before they were heated to 550 °C at a rate of 2 °C min^{-1} under helium (99.99 %, flow rate 60 mL min^{-1}). Differential scanning calorimetry (DSC) was performed with a Mettler DSC 822e that was cooled by an immersion cooler and purged with N_2. Structural and morphological analyses of the composites and the fillers were carried out by Electron Scanning Microscopy on a FEI Quanta 200 FEG-ESEM at 8–10 kV (low vacuum mode) and a working distance of 10 mm. Values for the average lengths (the longest dimension) of the aggregates in each sample are based on the measurements of at least 200 aggregates.

Thermal conductivity of the composites was measured using a C-Therm TCi™ Thermal Conductivity Analyzer by C-Therm. The TCi™ is based on a modified transient plane source technique and uses a one-sided, interfacial, heat reflectance sensor that applies a constant heat source to the sample (circular area of 17 mm diameter) for short periods of time. Five measurements were carried out on one sample for each filler material and average values are reported together with their percent relative standard deviations.

Results and discussion

Polyurethane [12, 15, 18–22] samples were prepared by mixing Desmodur® HL BA as isocyanate component with TEG as alcohol component in a 1:1 ratio of NCO and OH groups (see experimental part and Scheme 1).

Thermal analysis

Thermal stability of the polymer composites was determined by thermal gravimetric (TG) analysis at a heating rate of 2 °C min^{-1} under He atmosphere. All samples show a mass loss of 0.5–2.5 % between 50 and 100 °C, which is attributed to remaining solvent (Fig. 1). Interestingly, the largest loss of 2.5 % is observed for **PU (ref)**

Scheme 1 Synthesis of **PU–Ag** composites

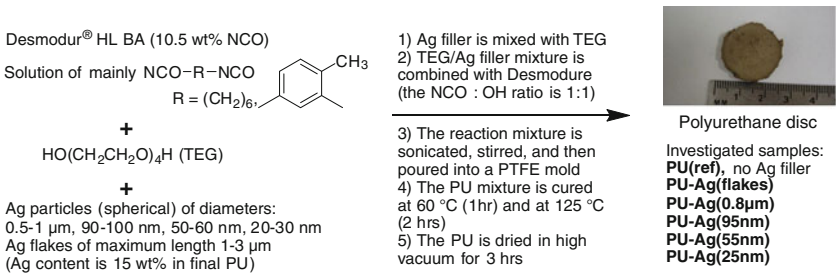

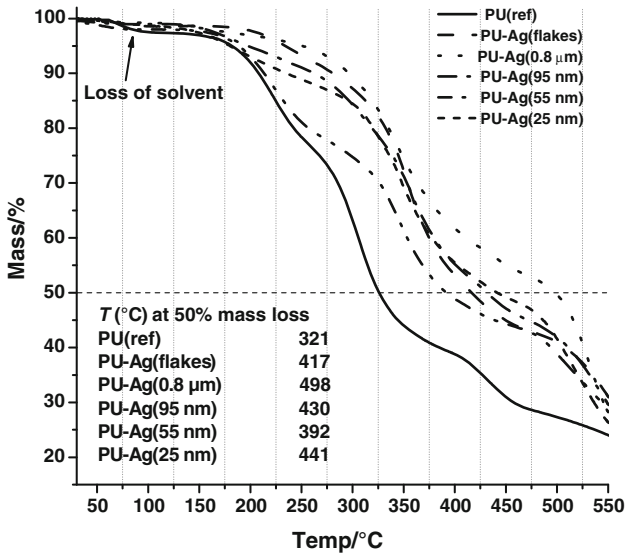

Fig. 1 TG analysis of PU samples heated to 550 °C under He at a rate of 2 °C min^{-1}

without Ag filler, while all composite mixtures lose only 0.5–1 %. This may be explained by the 15 wt% content of Ag particles that have a low affinity for ethyl acetate in comparison with PU and a competition between ethyl acetate and Ag filler for the available interaction sites of PU. Another reason could be the higher degree of crystallinity of the Ag composites as described later.

The onset of the next weight loss event varies between 125 (composites with Ag nanoparticles) and 165 °C (**PU–Ag (flakes)**) and initiates a set of at least three distinct weight loss events. Degradation of PU is known to take place in multiple steps and usually starts with the dissociation of urethane groups to the alcohol and isocyanate precursors and is followed by the decompositions of the formed precursor molecules [18, 23, 24].

The temperature at which 50 % mass loss has occurred is often provided for the comparison of thermal stabilities of polymers [12], and clearly indicates a higher thermal stability of the composite materials in comparison with **PU (ref)** (Fig. 1). Similar increase in stability have been observed for other PU composites that contain Ag and Au nanoparticles [12, 20], but our results also indicate that Ag fillers of micrometer size increase the thermal stability more than the nano-sized Ag particles. In fact, the smallest increase in $T_{50\%\ \text{loss}}$ is observed for **PU–Ag (55 nm)** (71 °C in comparison to **PU (ref)**) and the largest increase of 177 °C is observed for **PU–Ag (0.8 µm)**. The higher thermal stability of the composite materials is often explained with restricted motions of the polymer chains and the formation of more crystalline domains in the matrix [12, 15]. DSC measurements were conducted to probe differences in the degree of crystallinity between the different PU materials. All the samples show similar thermal behavior and undergo broad glass and melting transitions between −30 and 180 °C in the first heating run (Table 1). Only glass transitions are observed in the second and subsequent heating runs at a heating rate of 10 °C/min and a cooling rate of 5 °C/min (Table 2).

Table 1 Transition temperatures and enthalpies measured by DSC under N_2 at a heating rate of 10 °C min^{-1} and a cooling rate of 5 °C min^{-1}

Compound	T_g/°C	$T_{melting}$/°C (onset, peak, end point)	ΔH/Jg^{-1}
PU (ref)	−24	25, 92, 170	15.24
PU–Ag (flakes)	−3	(20), 71, 135	31.34
PU–Ag (0.8 µm)	33	(10), 75, 180	39.85
PU–Ag (95 nm)	−5	(10), 77, 140	37.35
PU–Ag (55 nm)	21	(10), 69, 160	35.25
PU–Ag (25 nm)	12	(−5), 58, 105	28.76

T_g was measured in the second heating run to avoid overlap between glass and melting transitions. Values in brackets are approximated because glass and melting transitions overlap

Table 2 Average maximum dimensions of Ag aggregates in cured PU composites measured by SEM (at least 200 aggregates were counted for each sample)

Sample	Average aggregate dimensions/µm
PU–Ag (flakes)	1.8 ± 0.6
PU–Ag (0.8 µm)	3.9 ± 2.0
PU–Ag (95 nm)	1.1 ± 0.6
PU–Ag (55 nm)	1.22 ± 0.7
PU–Ag (25 nm)	1.3 ± 0.9

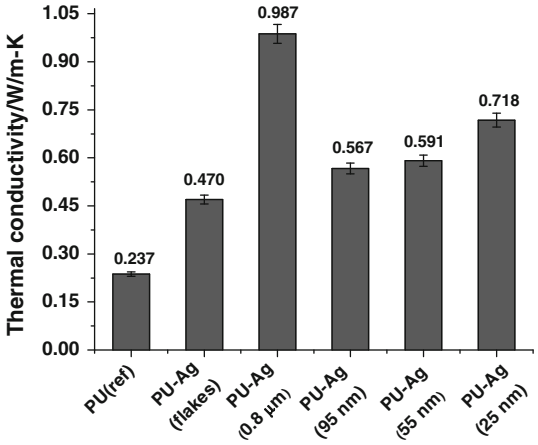

Fig. 2 Thermal conductivity of **PU (ref)** and **PU–Ag** composites. *Error bars* represent the % relative standard deviation of five measurements on the same sample

The glass transition temperatures of **PU–Ag** composites move to higher temperatures by at least 20 °C in comparison with **PU (ref)**. This change is mainly a result of significantly broader glass transitions in the composite materials and may be reasoned with a larger number of different environments for the polymer chains. In contrast, the melting transitions of the composites decrease by at least 15 °C while their melting enthalpies increase by 100–130 % in comparison to **PU (ref)**. An increase in melting enthalpies, which is equivalent to a higher degree of crystallinity, is often observed in polymer composite materials because more nucleation sites are available [12, 15]. The observed decrease in melting temperatures of the **PU–Ag** composites in comparison to **PU (ref)** can be reasoned with the formation of significantly smaller crystallites but was not investigated in more detail.

A comparison of the PU composite materials containing spherical Ag particles reveals a decrease of their degree of crystallinity with decreasing size of the particles. This is contrary to our expectation because at an equal content of Ag by mass the smaller particles should be present at larger numbers and provide more nucleation sites. A higher degree of aggregation may reduce the number of nucleation sites, but the largest aggregates are formed by the largest spherical Ag particles in **PU–Ag (0.8 µm),** and this sample also displays the highest degree of crystallinity. Clearly, other parameters such as the shapes of particles and aggregates and the structure of their surfaces must also affect the crystallization of the PU matrix. However, the DSC data agree with the thermal stability measured by TG analysis as the most crystalline material **PU–Ag (0.8 µm)** is also the thermally most stable.

Thermal conductivity and microstructural analysis

Thermal conductivity of the PU disks was measured by a modified transient plane source technique [25, 26]. The values range between 0.2 and 1.0 W/m–K and agree well with previously reported values for PU composites [17]. Expectedly, the thermal conductivity of **PU (ref)** is the lowest with 0.237 W/m–K. The addition of 15 wt% Ag filler increased the thermal conductivity of PU composites by factors between 2 and 4 (Fig. 2). The smallest increase in thermal conductivity is observed in **PU–Ag (flakes)** whereas composite **PU–Ag (0.8 µm)** shows the largest increase by a factor of 4.2. All the PU composites filled with Ag nanoparticles showed thermal conductivities in-between those of **PU–Ag (flakes)** and **PU–Ag (0.8 µm)**. Interestingly, among nano-sized Ag fillers, the thermal conductivity increases with decreasing size of the Ag nanoparticles (**PU–Ag (25 nm)** > **PU–Ag (55 nm)** > **PU–Ag (95 nm)**).

To better understand the observed differences in thermal conductivity, both aggregation of the particles and their distribution in the PU matrix were studied by SEM (Fig. 3).

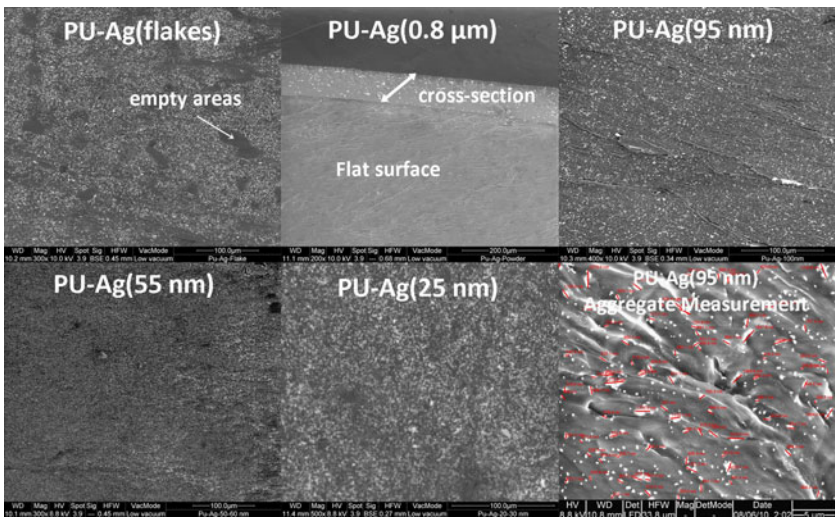

Fig. 3 SEM micrographs of PU composites. All images are the top surface morphologies while **PU–Ag (0.8 µm)** shows both cross section and top surface of the disk. No differences in filler distribution at the cross-section or at the top surface were observed. Aggregate measurements are exemplarily shown for **PU–Ag (95 nm)**. Images are generated from signals of backscattered electrons (**PU–Ag (flakes)**, **PU–Ag (95 nm)**, **PU–Ag (25 nm)**) or combined signals of backscattered and secondary electrons

The average aggregate size was determined by measuring the longest dimension of each aggregate and averaging over at least 200 aggregates observed in the SEM images. The results given in Fig. 3 clearly show a decrease in aggregate size for spherical Ag filler in the order **PU–Ag (0.8 μm) > PU–Ag (25 nm) > PU–Ag (55 nm) > PU–Ag (95 nm)**, which qualitatively agrees with the observed decrease in thermal conductivity. It is likely that the higher thermal conductivity of samples with larger aggregates of more fractal or elongated shapes results from a better overall connectivity between the conductive filler in the PU matrix, which agrees with what has been proposed by Evans et al. [10].

However, just based on aggregate size (1.8 μm actually is the length of individual flakes) sample **PU–Ag (flakes)** should show the second highest thermal conductivity and not the lowest as observed. This discrepancy may be explained with the stacking of the flake-shaped particles, which is a type of aggregation that does not significantly increase the size of aggregates. The presence of empty areas in **PU–Ag (flakes)** also reveals an uneven distribution of the flakes and their aggregates that generates a less connected structure of the filler in the PU matrix. In contrast, distributions of spherical Ag particles appear to be uniform and independent of their different sizes.

Differences in thermal interfacial resistance, often referred to as Kapitza resistance, may also affect the thermal conductivity of the composites but are assumed to be comparatively small because the interfaces between Ag/Ag_2O surfaces and the PU should be rather similar in all composites and the thermal conductivity of silver and silver oxide is similar with 400–430 W/mK [4].

Conclusions

PU–Ag composites were prepared from Desmodur® and a suspension of Ag filler in TEG. All tested Ag fillers increase the thermal stability and conductivity of the PU composites in comparison to a reference sample that does not contain Ag filler (**PU (ref)**), but the highest increases are obtained for spherical Ag particles of 0.5–1.0 μm size. Among spherical particles, increases in thermal conductivity correlate with increases in average aggregate size, but the thermal conductivity of **PU–Ag (flakes)** is the lowest although its aggregates are the second largest. This discrepancy is explained with the flake-shape of the Ag filler that generates aggregates of stacked flakes and a less uniform distribution in the PU matrix, which result in insignificant increases in aggregate size in comparison with the individual flakes and in an inhomogeneous filler network, respectively.

References

1. Luedtke A. Thermal management materials for high-performance applications. Adv Eng Mater. 2004;6(3):142–4.
2. Ong B, Chow SG, Tang E. Thermally enhanced, next-generation 3-D power packages: a heat-management solution. Adv Packaging. 2005;14(11):23–5.
3. Zweben C. Advances in composite materials for thermal management in electronic packaging. JOM. 1998;50(6):47–51.
4. Zweben C. High-performance thermal management materials. Adv Packaging. 2006;15(2):20–2.
5. Zweben CH. Advances in high-performance thermal management materials: a review. J Adv Mater. 2007;39(1):3–10.
6. Bulsara M, Celler G, White T, Standley B, Huff H. Roadmap requirements for emerging materials. Solid State Technol. 2006; 49(1):34–8.
7. Fletcher LS. A review of thermal enhancement techniques for electronic systems. IEEE T Compon Hybr. 1990;13(4):1012–21.
8. Zweben C. Advanced thermal management materials for electronics and photonics. Adv Microelectron. 2010;37(4):14–9.
9. Saums D, Jarrett B, Mackie AC, Ross J. Thermal management materials choices for power semiconductors. Adv Microelectron. 2009;36(4):8–16.
10. Evans W, Prasher R, Fish J, Meakin P, Phelan P, Keblinski P. Effect of aggregation and interfacial thermal resistance on thermal conductivity of nanocomposites and colloidal nanofluids. Int J Heat Mass Tran. 2008;51(5–6):1431–8.
11. Xingyi H, Pingkai J, Liyuan X. Ferroelectric polymer/silver nanocomposites with high dielectric constant and high thermal conductivity. Appl Phys Lett. 2009;95(24):242901.
12. Chou CW, Hsu SH, Chang H, Tseng SM, Lin HR. Enhanced thermal and mechanical properties and biostability of polyurethane containing silver nanoparticles. Polym Degrad Stabil. 2006;91(5):1017–24.
13. Kim JY. Amphiphilic polyurethane-co-polystyrene network films containing silver nanoparticles. J Ind Eng Chem. 2003;9(1):3 7–44.
14. Chen S, Sui J, Chen L. Positional assembly of hybrid polyurethane nanocomposites via incorporation of inorganic building blocks into organic polymer. Colloid Polym Sci. 2004;283(1): 66–73.
15. Chou CW, Hsu SH, Wang PH. Biostability and biocompatibility of poly(ether)urethane containing gold or silver nanoparticles in a porcine model. J Biomed Mater Res A. 2008;84(3):785–94.
16. Dallas P, Sharma VK, Zboril R. Silver polymeric nanocomposites as advanced antimicrobial agents: classification, synthetic paths, applications, and perspectives. Adv Colloid Interfac. 2011;166(1–2): 119–35.
17. Raja M, Shanmugharaj AM, Ryu SH, Subha J. Influence of metal nanoparticle decorated CNTs on polyurethane based electro active shape memory nanocomposite actuators. Mater Chem Phys. 2011;129(3):925–31.
18. Lin M-F, Tsen W-C, Shu Y-C, Chuang F-S. Effect of silicon and phosphorus on the degradation of polyurethanes. J Appl Polym Sci. 2001;79(5):881–99.
19. Hsu SH, Tseng HJ, Lin YC. The biocompatibility and antibacterial properties of waterborne polyurethane-silver nanocomposites. Biomater. 2010;31(26):6796–808.
20. S-h Hsu, Chou C-W. Enhanced biostability of polyurethane containing gold nanoparticles. Polym Degrad Stabil. 2004;85(1): 675–80.
21. Hung HS, Hsu SH. Biological performances of poly(ether)urethane-silver nanocomposites. Nanotechnology. 2007;18(47):475101–10.
22. Petrie EM. Handbook of adhesives and sealants. 2nd ed. New York: McGraw-Hill; 2007.

23. Rwei S-P, Wang L. Synthesis and electrical, rheological and thermal characterization of conductive polyurethane. Colloid Polym Sci. 2007;285(12):1313–9.
24. Erickson K. Thermal decomposition mechanisms common to polyurethane, epoxy, poly(diallyl phthalate), polycarbonate and poly(phenylene sulfide). J Therm Anal Calorim. 2007;89(2): 427–40.
25. Wang S, Liang R, Wang B, Zhang C. Dispersion and thermal conductivity of carbon nanotube composites. Carbon. 2009;47(1): 53–7.
26. Sun Y, Sheng P, Di C, Jiao F, Xu W, Qiu D, Zhu D. Organic thermoelectric materials and devices based on *p*- and *n*-type poly(metal 1,1,2,2-ethenetetrathiolate)s. Adv Mater. 2012;24(7):932–7.